
Supporting information

**Development of a novel theory of pressure-induced
nucleation in supercritical carbon dioxide**

Qi-Bo Wang, Qin-Qin Xu*, Jian-Zhong Yin, Hong-Yue Zhu, Bao-Lin Liu,
Ming-Zhe Yang

State Key Laboratory of Fine Chemicals, School of Chemical Engineering,

Dalian University of Technology, Dalian 116024, China

Table S1 Data of $\text{MoO}_2(\text{acac})_2$ mole fraction y_1 in scCO_2

| Temperature (°C) | Pressure (MPa) | Density of scCO_2 ($\text{kg}\cdot\text{m}^{-3}$) | $y_1 \times 10^4$ |
|---------------------|-------------------|---|-------------------|
| 40 | 7.4 | 233.38 | 1.818 |
| | 10.0 | 631.74 | 0.809 |
| | 12.0 | 719.38 | 1.033 |
| | 14.4 | 764.47 | 1.236 |
| | 16.0 | 795.91 | 1.315 |
| | 18.0 | 820.39 | 1.485 |
| | 20.0 | 840.61 | 1.604 |
| 50 | 7.4 | 188.78 | 1.420 |
| | 10.6 | 460.74 | 1.350 |
| | 12.0 | 587.07 | 2.026 |
| | 14.0 | 673.7 | 2.535 |
| | 16.0 | 723.27 | 2.894 |
| | 18.0 | 758.11 | 3.754 |
| | 20.0 | 785.16 | 4.172 |
| 60 | 7.4 | 168.75 | 1.316 |
| | 10.0 | 290.81 | 1.821 |
| | 12.0 | 436.26 | 2.006 |
| | 14.0 | 563.09 | 2.830 |
| | 16.0 | 638.84 | 3.761 |
| | 18.0 | 688.34 | 4.128 |
| | 20.0 | 724.63 | 4.829 |

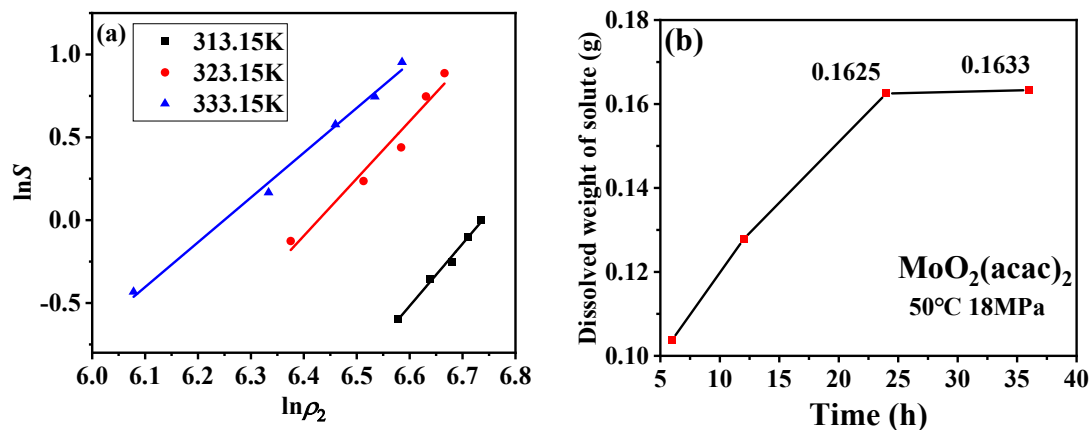


Fig. S1 (a) Linear relationships between the logarithms solubility and the logarithms density of scCO₂ at various temperatures. (b) Relationships between dissolution time and dissolved weight of solute at 50°C, 18.0 MPa.

Linear relationships between the logarithms solubility and the logarithms density of scCO₂ were obtained at various temperatures when $p \geq 12.0$ MPa, as shown in Fig.S1(a). The solubility at 323.15 K and 333.15 K was higher than that at 313.15 K, which indicated that temperature played a dominant factor in solubility at high density.

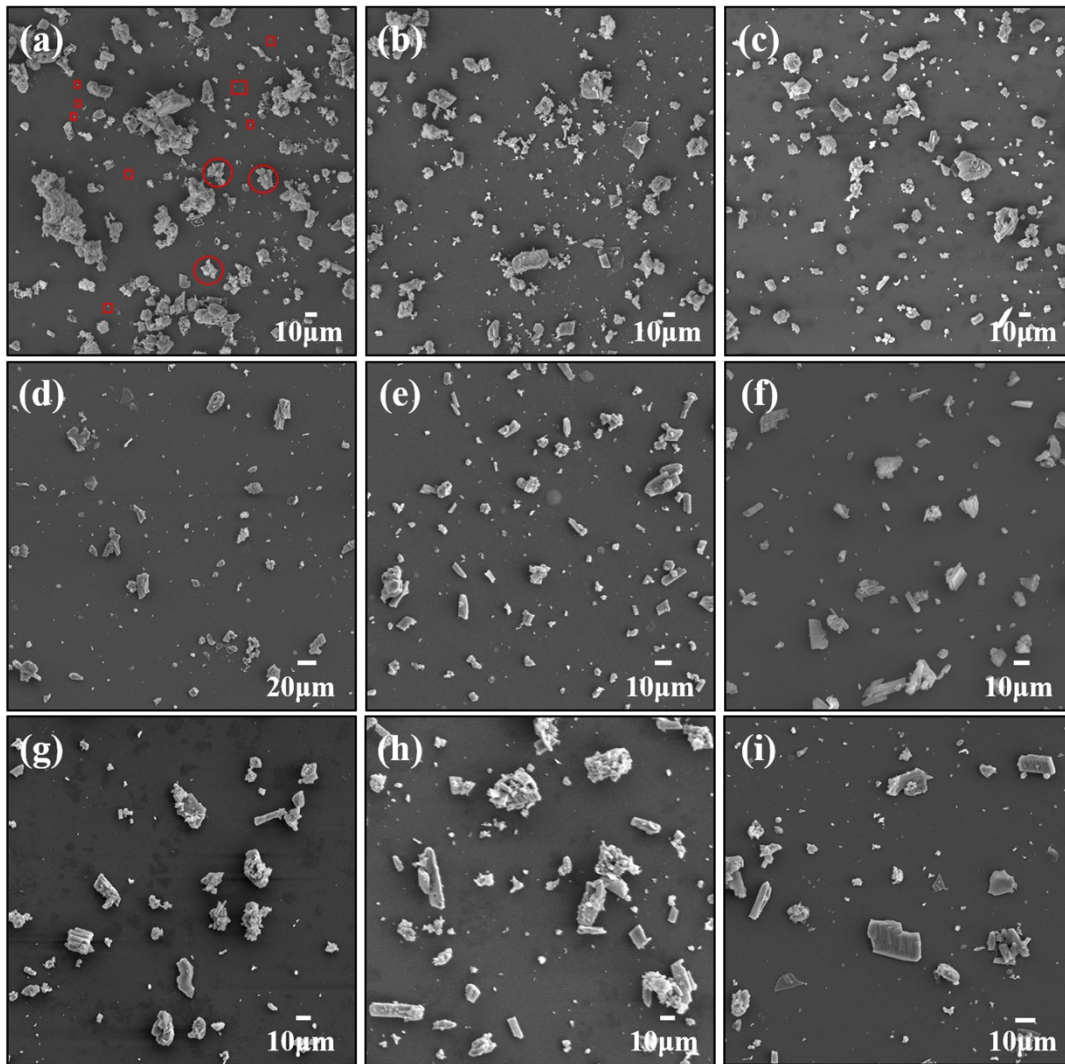


Fig.S2 SEM images of $\text{MoO}_2(\text{acac})_2$ particles obtained by PI-SCPN process at $p=20.0$ MPa, various temperatures and supersaturation. (a) $T=333.15$ K, $\sigma_c=12$; (b) $T=333.15$ K, $\sigma_c=8$; (c) $T=333.15$ K, $\sigma_c=5$; (d) $T=323.15$ K, $\sigma_c=12$; (e) $T=323.15$ K, $\sigma_c=8$; (f) $T=323.15$ K, $\sigma_c=5$; (g) $T=313.15$ K, $\sigma_c=12$; (h) $T=313.15$ K, $\sigma_c=8$; (i) $T=313.15$ K, $\sigma_c=5$.

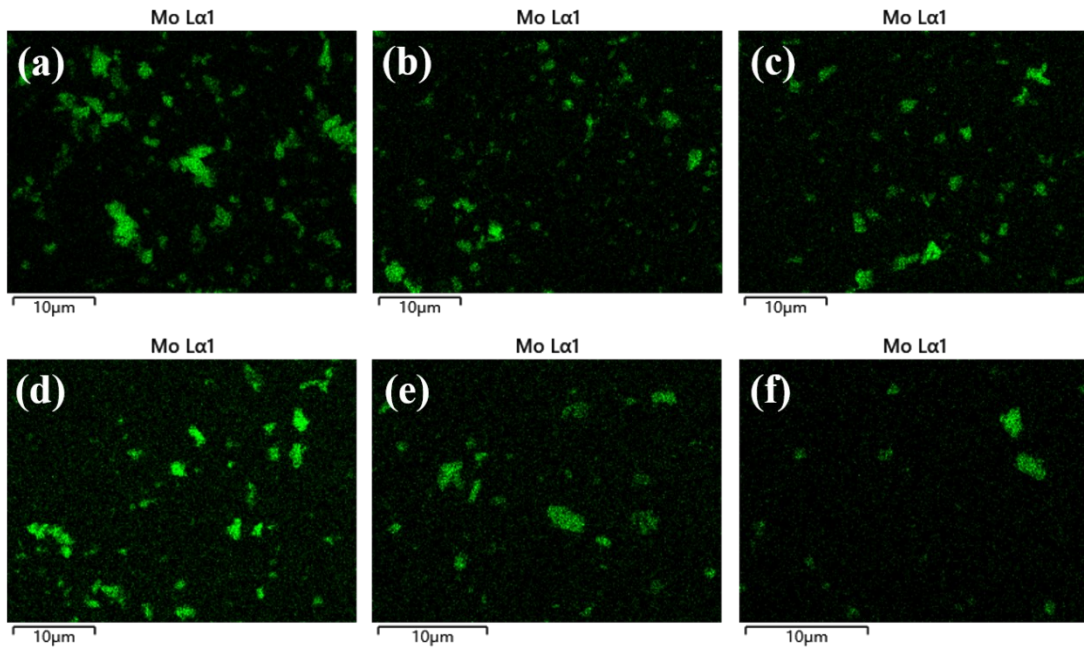


Fig. S3 EDS images of some samples (a) Sample 1, $T=333.15$ K, $p=20.0$ MPa, $\sigma=12$; (b) Sample 3, $T=333.15$ K, $p=20.0$ MPa, $\sigma=5$; (c) Sample 6, $T=323.15$ K, $p=20.0$ MPa, $\sigma=5$; (d) Sample 7, $T=313.15$ K, $p=20.0$ MPa, $\sigma=12$; (e) Sample 9, $T=313.15$ K, $p=20.0$ MPa, $\sigma=5$; (f) Sample 12, $T=323.15$ K, $p=14.0$ MPa, $\sigma=5$.

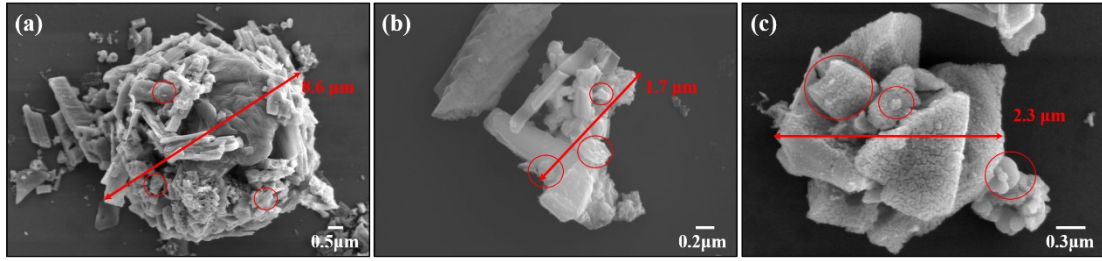


Fig. S4 SEM images of agglomerated particles at various operating conditions (a) $T=333.15$ K, $p=20.0$ MPa, $\sigma=12$; (b) $T=323.15$ K, $p=20.0$ MPa, $\sigma=5$; (c) $T=313.15$ K, $p=20.0$ MPa, $\sigma=12$.

In Fig. S4, the size of the agglomerated structure was significantly larger than that of a cluster. The red circle contained at least one cluster.

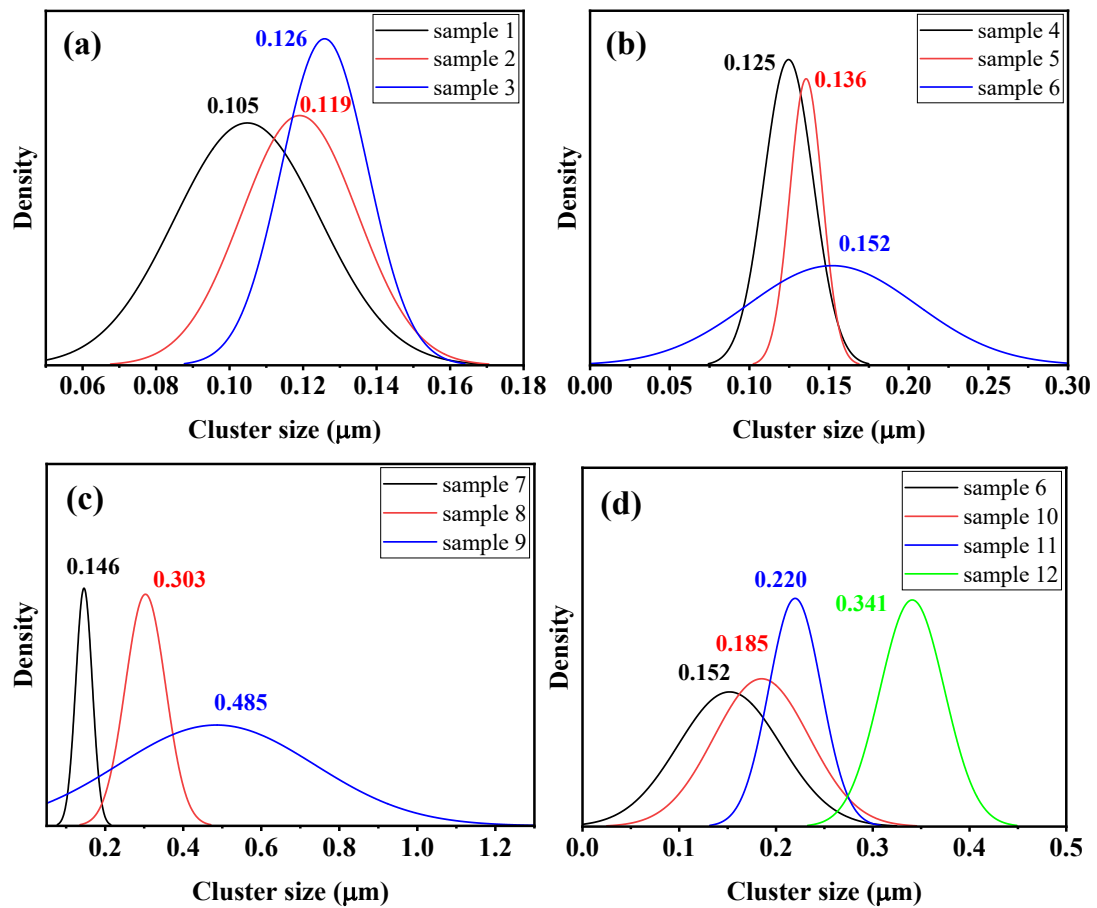


Fig. S5 Statistical distribution of cluster size r at various conditions. (a) samples 1, 2, and 3; (b) samples 4, 5, and 6; (c) samples 7, 8, and 9; (d) samples 6, 10, 11, and 12.

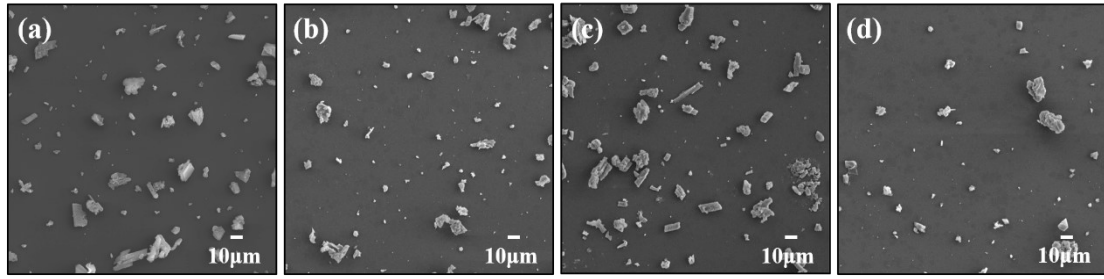


Fig. S6 SEM image of Cluster at $T=323.15$ K, $\sigma_c = 5$ and various pressure;

(a) $p=20.0$ MPa; (b) $p=18.0$ MPa; (c) $p=16.0$ MPa; (d) $p=14.0$ MPa.